Published in final edited form as:
J Neurochem. 2013 June ; 125(6): 822–831. doi:10.1111/jnc.12246.

Intracellular Dialysis Disrupts Zn^{2+} Dynamics and Enables Selective Detection of Zn^{2+} Influx in Brain Slice Preparations

Isamu Aiba[1], **Adrian K West**[2], **Christian T Sheline**[3], and **C. William Shuttleworth**[1]

[1]Department of Neurosciences, University of New Mexico, Albuquerque, NM, USA

[2]NeuroRepair Group, Menzies Research Institute, University of Tasmania, Hobart, Australia

[3]Department of Ophthalmology and the Neuroscience Center of Excellence LSU Health Sciences Center, New Orleans, LA, USA

Abstract

We examined the impact of intracellular dialysis on fluorescence detection of neuronal intracellular Zn^{2+} accumulation. Comparison between two dialysis conditions (standard; 20minutes, brief; 2minutes) by standard whole-cell clamp revealed a high vulnerability of intracellular Zn^{2+} buffers to intracellular dialysis. Thus low concentrations of zinc-pyrithione generated robust responses in neurons with standard dialysis, but signals were smaller in neurons with short dialysis. Release from oxidation-sensitive Zn^{2+} pools were reduced by standard dialysis, when compared with responses in neurons with brief dialysis. The dialysis effects were partly reversed by inclusion of recombinant metallothionein-3 in the dialysis solution. These findings suggested that extensive dialysis could be exploited for selective detection of transmembrane Zn^{2+} influx. Different dialysis conditions were then used to probe responses to synaptic stimulation. Under standard dialysis conditions, synaptic stimuli generated significant FluoZin-3 signals in wild-type (WT) preparations, but responses were almost absent in preparations lacking vesicular Zn^{2+} (ZnT3-KO). In contrast, under brief dialysis conditions, intracellular Zn^{2+} transients were very similar in WT and ZnT3-KO preparations. This suggests that both intracellular release and transmembrane flux can contribute to intracellular Zn^{2+} accumulation after synaptic stimulation. These results demonstrate significant confounds and potential use of intracellular dialysis to investigate intracellular Zn^{2+} accumulation mechanisms.

Keywords

hippocampal slice; whole-cell; metallothionein; ZnT3; pyrithione; Zinc

INTRODUCTION

Zn^{2+} is an essential ion required for a wide range of functions in mammalian cells. While total intracellular Zn^{2+} content is quite high (>200 μM), cytoplasmic free Zn^{2+} concentrations are maintained at extremely low levels (<1 nM), due to the fact that much is bound in structural proteins and also the high activities of intracellular buffer and transporter systems (Colvin et al., 2008; West et al., 2008; Sensi et al., 2009). However cytosolic Zn^{2+} transients appear to be important for intracellular signaling. For example, elevated cytoplasmic free Zn^{2+} levels in neurons have been implicated to modulation of neuronal

Correspondence to: CW Shuttleworth, Ph.D., Department of Neurosciences, University of New Mexico School of Medicine, Albuquerque, NM 87131-0001, Phone (505) 272 4290, Fax (505) 272 8082, bshuttleworth@salud.unm.edu.

The Authors declare that there is no conflict of interest.

circuit activity, and activation of neurotoxic pathways when intracellular Zn^{2+} levels become excessively high (Choi and Koh, 1998; Frederickson et al., 2005).

In the mammalian brain, Zn^{2+} is highly concentrated in synaptic vesicles of glutamergic neurons, due to the activity of the vesicular Zn^{2+} transporter ZnT3 (Cole et al., 1999). Vesicular Zn^{2+} can be released as a neuromodulator and can directly modify the function of ion channels and receptors via direct interactions. In addition to extracellular actions, released Zn^{2+} may also translocate into postsynaptic neurons and potentially contribute to plasticity of some synapses (Huang et al., 2008). Glutamate exposures have been widely used to study neuronal intracellular Zn^{2+} homeostasis (Sensi et al., 2002; Sensi et al., 2003; Dineley et al., 2008; Kiedrowski, 2011) and activation of NMDA-type glutamate receptors (NMDARs) have been shown to release Zn^{2+} from intracellular pools. Synaptic Zn^{2+} release and influx has been reported to contribute to postsynaptic Zn^{2+} accumulation (Suh, 2009), however there is not yet evidence for liberation from intracellular stores by endogenous glutamate release. The relative contributions of these two Zn^{2+} sources following synaptic stimulation remain to be clarified, as does the impact of standard electrophysiological recording methods on intracellular Zn^{2+} signals.

The whole-cell clamp recording technique results in substantial dialysis of the intracellular compartment, due to large differences in pipette and intracellular volumes ($>10^{-6}$ vs $10^{-10\sim12}$ liter). Due to effective washout of some intracellular components, intracellular dialysis can lead to rundown of Ca^{2+} currents (Sakmann and Neher, 1984) and mask important neurophysiological responses such as long-term potentiation (Malinow and Tsien, 1990). Zn^{2+} signaling to NMDARs has also been shown to be disrupted by extended dialysis in cultured cortical neurons (Manzerra et al., 2001). On the other hand, intracellular dialysis has been also exploited as a valuable method to manipulate intracellular constituents (Blatow et al., 2003; Eggermann and Jonas, 2012). Whether or not whole-cell recording depletes neurons of important Zn^{2+} buffers and/or otherwise modifies detection of intracellular Zn^{2+} responses has not been explicitly tested.

In the present study, we demonstrate a significant vulnerability of intracellular Zn^{2+} buffers and/or pools to intracellular dialysis. While these dialysis methods may be a significant technical confound, we also demonstrate that they can be exploited to evaluate contributions of both synaptic and intracellular Zn^{2+} release, following synaptic stimulation.

METHODS

1. Slice preparation

All procedures using experimental animals were approved by the Institutional Animal Care and Use Committee of the University of New Mexico. Brain slices were prepared from 4–10 week old WT and ZnT3 KO C57BL/6 animals of both sexes. Data in each specific experiment were collected from matched numbers of each sex, within an age range of 2 weeks. ZnT3 KO animals were originally developed by (Cole et al., 1999) and backcrossed onto the C57BL/6 line for at least 13 generations. Both WT and ZnT3 KO homozygote colonies were established and maintained at the University of New Mexico.

Mice were deeply anesthetized with a subcutaneous injection (0.2 ml) of ketamine/xylazine mix (85 mg/ml and 15 mg/ml, respectively) and decapitated. Brains were carefully extracted into ice-cold cutting solution (in mM: 220 sucrose, 1.25 NaH_2PO_4, 25 $NaHCO_3$, 3 KCl, 10 glucose, 0.2 $CaCl_2$, 6 $MgSO_4$ equilibrated with 95% O_2/5% CO_2 gas), hemisected and sliced at 350 μm thickness with a vibratome. Slices were allowed to recover in ACSF (in mM: 124 NaCl, 1.25 NaH_2PO_4, 25 $NaHCO_3$, 3 KCl, 2 $CaCl_2$, 1 $MgSO_4$ 10 glucose equilibrated with 95% O_2/5% CO_2 mix-gas) for 1 hour at 35°C, and were subsequently maintained at room

temperature in ACSF. Slices were transferred to a recording chamber (RC-27, Warner Instruments) and superfused with ACSF at 2 mm/min and 32°C.

2. Zn^{2+} indicator loading into single CA1 neurons

Intracellular Zn^{2+} dynamics were evaluated by using the high affinity indicator Fluo-Zin3, loaded via whole cell dialysis into single CA1 pyramidal neurons. Neurons were visually identified, and patch pipettes (3–5 MΩ) contained (in mM): 135 potassium gluconate, 8 NaCl, 1 $MgCl_2$, 2 Na_2ATP, 0.3 NaGTP, 10 Hepes, 0.05 EGTA. pH was adjusted to 7.2 with KOH and FluoZin-3 added to the pipette solution.

A central issue in this study was the influence that whole-cell dialysis had on intracellular Zn^{2+} dynamics. Therefore the duration of dialysis was carefully monitored, and the electrode withdrawn from the neuron at specified times after the initial establishment of the whole-cell configuration. Thus membrane rupture was determined as the time when initial access resistances dropped below 30 MΩ, and if this was not completed within 10 seconds of initial attempts, the neuron was discarded. During intracellular dialysis, neurons were voltage clamped at −65 mV (holding current range between −50 and +50 pA), and the quality of whole-cell configuration was monitored based on the holding current and membrane response to test pulse (−5 mV, 100 ms). Neurons were discarded when holding current exceeded −100 pA for more than 20 s without any sign of recovery, or when series resistance exceeded 30 MΩ. Following intracellular dialysis, the loading pipette was carefully withdrawn. Successful electrode withdrawal was determined by formation of an out-side-out recording configuration, and could be achieved within 20 seconds. After successful electrode withdrawal, neurons were allowed 20 minutes recovery, prior to onset of any stimulation.

The concentration of FluoZin-3 added to the pipette solution depended on the duration of dialysis, in order to approximately match the final FluoZin-3 concentration achieved in neurons (see Figure 1). The tested concentration ranged from 40–500 μM (see Results).

In some experiments, recombinant human metallothionein-3 (MT3) was added to the intracellular solution. This was supplied as lyophilized purified recombinant human MT3, present as a mixture of Zn^{2+}-bound forms (approximately 80% Zn_7MT3, 10% of Zn_6MT3 and 10% Zn_8MT3 (Bestenbalt LLC, Tallinn, Estonia)). A 5 μM MT3 stock solution was prepared as a 10-times concentrated pipette solution lacking ATP/GTP, and including 10% chelex resin (v/v, Chelex 100, Bio-Rad, CA). Chelex is an ion exchange resin and was used here to remove weakly-bound Zn^{2+} from metallothionein as demonstrated previously (Krezoski et al., 1988). This stock was stored at −80°C, and MT3 and ATP/GTP were then added to the pipette solution immediately prior to experiments

3. Fluorescence imaging

FluoZin-3 fluorescence was excited with 495 nm light (120 ms) delivered from monochromator via a dichoric mirror (505 nm long pass). Emission signals were band-passed filtered (535/50 nm) and acquired using a CCD camera (Till Imago) controlled by Till Vision software (version 4.04). Intracellular fluorescence signals were calculated after subtracting background neuronal autofluorescence within the same images. Intracellular basal Zn^{2+} concentrations were estimated from the equation described in (Grynkiewicz et al., 1985): $[Zn^{2+}] = K_d (F - F_{min})/(F_{max} - F)$, where K_d=15nM (Gee et al., 2002), F_{max} was obtained after exposure to a saturating concentration of ZnPyr (see Figure 1B), and F_{min} was determined from TPEN exposures to be zero.

Because of the high signal to noise ratio achieved by single-cell loading with FluoZin-3, intracellular fluorescence values could be approximated by the maximum fluorescence

values obtained from low-pass filtering (3×3 pixel averaging) images. The kinetics of responses were analyzed as changes relative to the basal fluorescence intensities. In some experiments (e.g. Figure 1 100 μM ZnPyr exposures), significant tissue swelling occurred and focus adjustment was required.

4. Synaptic stimulation

Synaptic responses were evoked with a concentric bipolar stimulating electrode placed >100 μm from the imaging site. Glass recording electrodes filled with ACSF (0.5–1 MΩ) were placed adjacent to neurons being imaged in order to verify activation of postsynaptic neurons near the recording sites. In each experiment, input-output curve were generated based on field excitatory postsynaptic potentials (fEPSP) evoked with single current pulses (70 μs, 0.1 Hz). 70% maximum stimulation was used for test stimuli. In all experiments, input-output curves were determined at least 10 minutes after recovery of neurons from indicator loading and removal of the filling electrode.

5. Reagents

Unless otherwise noted, all chemicals were from Sigma Aldrich (St Louis MO). FluoZin-3 and TPEN (N,N,N′,N′-Tetrakis(2-pyridylmethyl)ethylenediamine were obtained from Life Technologies (Carlsbad, CA). As noted above, recombinant MT3 was from Bestenbalt LLC, Tallinn, Estonia.

6. Statistical Analysis

All statistical tests were performed by using Graph Pad Prism software (GraphPad Software, Inc., version 4.03). One-way ANOVA with post hoc Newman-Keuls multiple comparison tests were used throughout. Values are presented as mean +/− SEM. n values indicate numbers of cells tested. A p-value <0.05 was considered to be statistically significant.

RESULTS

1. Intracellular dialysis increased detection of intracellular Zn^{2+} increases

We first examined the hypothesis that intracellular dialysis could reduce intracellular Zn^{2+} buffering capacity, and make cytosolic Zn^{2+} increases more readily detectable. The general experimental approach is shown in Figure 1, where single pyramidal neurons were dialyzed via a conventional whole-cell patch pipette containing the membrane-impermeable Zn^{2+} indicator FluoZin-3. Two different durations of dialysis were compared (2 minutes and 20 minutes), and the concentration of indicator added to the pipette solution adjusted (500 μM and 40 μM, respectively) so that the final neuronal indicator concentrations were approximately matched. This was confirmed by exposing the indicator-loaded neurons with saturating concentration of ZnPyr (100 μM $ZnCl_2$, 5 μM sodium pyrithione, 20 minutes exposure) and obtaining maximum fluorescence signals (Figure 1A&B). The approximate intracellular Zn^{2+} concentrations were estimated by using an equation described in (Grynkiewicz et al., 1985), and the calculation confirmed extremely low resting intracellular Zn^{2+} concentrations (Figure 1C). These initial experiments verified that initial FluoZin-3 concentrations were closely matched in the neuronal populations, despite very different dialysis durations.

Figure 2 shows that the duration of dialysis had a substantial effect on the amplitude of Zn^{2+} increases detected by FluoZin-3, when neurons were challenged with a low concentration of zinc pyrithione (ZnPyr: 1 μM $ZnCl_2$ and 1 μM sodium pyrithione). Pyrithione serves to facilitate Zn^{2+} passage across the plasma membrane, and thereby increase intracellular Zn^{2+} levels independent of active transport mechanisms. As shown in Figure 2A, the FluoZin-3 response in the briefly dialyzed neurons was barely detectable, whereas large FluoZin-3

increases were detected in all neurons that were first subjected to standard (20 minutes) dialysis (Figure 2B). The increased signals with standard dialysis could be due to washout of an endogenous Zn^{2+} buffer into the dialysis pipette, and/or changes in transport mechanisms involved in accumulation and clearance.

Experiments in Figure 2C show that supplementation of the pipette solution with recombinant MT3 (0.5 μM) was sufficient to abolish the large Zn^{2+} signals seen with standard dialysis. The recombinant MT3 protein was initially supplied as a mixture of Zn^{2+} bound forms that is expected to retain significant Zn^{2+} binding capacity, as well as potentially providing a source of Zn^{2+} (see Methods and Discussion). We estimated relevant intracellular MT concentrations from previous publications (Hidalgo et al., 1994; Colvin et al., 2008) and examined effects of a range of MT3 concentrations (0.1–5 μM) in an initial set of pilot studies. 0.5 μM MT3 was then chosen for subsequent experiments, as this concentration showed significant effects on intracellular Zn^{2+} responses while having little deleterious effect on the quality of whole-cell recordings.

Although the difference in the amplitudes of response could be affected by initial fluorescence or Zn^{2+} concentration, our estimates of maximum fluorescence values as well as near zero minimum fluorescence values (after TPEN exposure) suggested this was not the case (see Figure 1B&C). These observations imply that intracellular dialysis revealed larger FluoZin-3 signals due to increased cytoplasmic Zn^{2+} concentration available for detection by the indicator. Supplementation with recombinant MT3 is consistent with the possibility that washout of endogenous Zn^{2+} buffering proteins could underlie the effect, however it is emphasized that addition of excess endogenous buffer in these studies could mask other contributing mechanisms (see Discussion).

2. Intracellular dialysis also reduced oxidation dependent intracellular Zn^{2+} release

Previous work has shown that addition of a membrane-permeable oxidant effectively mobilizes Zn^{2+} from intracellular stores/binding proteins, and leads to increases in Zn^{2+} that can be detected by cytosolic indicators (Aizenman et al., 2000). We therefore examined whether dialysis leads to depletion of the size of the oxidation-sensitive intracellular Zn^{2+} pool. After a stable baseline was collected, neurons were exposed to 200 μM DTDP for 20 minutes. As shown in Figure 3, briefly dialyzed neurons showed a robust increase in FluoZin-3 signals. In contrast, FluoZin-3 signal responses were very small in neurons with standard dialysis, suggesting much smaller oxidation sensitive Zn^{2+} pools in these preparations. Intermediate Fluozin-3 responses were observed in neurons with standard dialysis supplemented with recombinant MT3. These results suggest that intracellular dialysis may deplete oxidation-sensitive Zn^{2+} pools, and addition of Zn^{2+} bound recombinant MT3 can provide a Zn^{2+} pool in dialyzed neurons.

3. Dialysis allows dissection of multiple sources of Zn^{2+} following synaptic stimulation

The results above suggest that differences in dialysis conditions could be used experimentally to manipulate the ability to preferentially detect transmembrane Zn^{2+} influx (with standard dialysis) and liberation from intracellular binding sites (with short dialysis). We next examined whether these experimental approaches could be exploited to assess the contributions of different Zn^{2+} sources to intracellular Zn^{2+} accumulation following synaptic stimulation.

This was done using trains of synaptic stimulation (20 Hz for 10 s), as this was suggested to be a physiologically relevant stimulation intensity in a recent study of tissue metabolism in a similar preparation (Hall et al., 2012). As shown in Figure 4, these stimuli provided reliable detection of post-synaptic Zn^{2+} accumulation. For these experiments, the slow Zn^{2+} chelator

CaEDTA (1 mM) was included in recording bath solution in order to prevent detection of contaminating Zn^{2+} (see (Qian and Noebels, 2005) and Discussion). Based on previous studies, exposure to 1 mM CaEDTA should have little effect on basal intracellular Zn^{2+} concentration (Lavoie et al., 2007), and leave a significant fraction of rapidly released Zn^{2+} available at synaptic clefts (Vogt et al., 2000; Pan et al., 2011). Under these stimulation and recording conditions, slow Zn^{2+} increases were completely abolished by pre-exposure to a cocktail of glutamate receptor antagonists (20 μM DNQX, 5 μM D-AP5, 10 min), in both standard dialysis and brief dialysis conditions (see Supplemental Figure).

Figure 4 shows a summary of intracellular Zn^{2+} responses of postsynaptic neurons, indicator loaded with standard dialysis, brief dialysis and standard dialysis with MT3. In order to evaluate contributions of synaptic Zn^{2+} release, experiments were compared between WT and ZnT3 KO preparations. Strong genotypic differences were seen in the standard dialysis preparations (Fig 4A&B). Thus WT preparations showed a robust FluoZin-3 signal increase peaked during 1–2 minutes after stimulation and slowly decayed over next 5 minutes, while responses was virtually absent in ZnT3 KO preparations (Fig 4A&B). These data suggest that the responses observed in dialyzed WT preparations were largely contributed to by presynaptic Zn^{2+} release, and are consistent with the possibility that significant depletion of intracellular Zn^{2+} buffering by standard dialysis facilitated detection of the response.

A large difference between WT and ZnT3 KO preparations was not seen in briefly dialyzed neurons. Thus both WT and ZnT3 KO preparation showed intracellular Zn^{2+} responses in these cells, following synaptic stimulation (Fig 4C&D). The responses in ZnT3 KO preparations raised the possibility that these responses were generated by liberation from intracellular sources.

Figures 4E&F show experiments to test whether artificial provision of an intracellular Zn^{2+} source and sink (by inclusion of MT3 in the pipette solution) could reveal additional Zn^{2+} release signals in neurons that had been extensively dialyzed. MT3 addition had no additional effect in WT neurons, but did reveal Zn^{2+} increases in ZnT3 KO neurons (compare Figures 4C&F).

Taken together, these results suggest that synaptic stimulation leads to postsynaptic Zn^{2+} accumulation from at least two sources, which can be preferentially demonstrated with different dialysis methods. Synaptic release can be readily demonstrated after standard dialysis, where a large portion of the Zn^{2+} buffering system is lost. In contrast, briefly-dialyzed neurons appear to retain a significant source of intracellular Zn^{2+}, which can generate postsynaptic FluoZin-3 signals, even in the absence of synaptically-released Zn^{2+}.

DISCUSSION

1. General

The present study examined effects of intracellular dialysis on Zn^{2+} measurements in neurons subjected to whole-cell recording in acute slice preparations. A main finding is that dialysis appears to effectively deplete intracellular Zn^{2+} buffering and decrease the size of oxidation-sensitive intracellular Zn^{2+} pools. Such disruption of intracellular Zn^{2+} homeostasis was shown to significantly modify detection of intracellular Zn^{2+} responses to a train of synaptic stimulation. Thus standard whole-cell dialysis facilitated detection of synaptic Zn^{2+} translocation, whereas in briefly-dialyzed preparations intracellular Zn^{2+} responses seem to be mediated mainly by intracellular Zn^{2+} liberation. Together, these findings indicate a high vulnerability of intracellular Zn^{2+} homeostasis to whole-cell dialysis, and demonstrate its potential use for selective detection of intracellular Zn^{2+} signals arising from different mechanisms.

2. Dialysis effects

The present study compared effects of two different durations of intracellular dialysis; one standard (20 minutes) and one intentionally very brief (2 minutes). It is generally understood that intracellular dialysis is one of the most profound confounds of whole-cell clamp recordings. Washout of intracellular constituents and the imposition of a homogenous intracellular ionic composition improves the resolution of electrophysiological recordings, however dialysis of channel subunits or signaling molecules can prevent recording of significant physiological responses (see Introduction). The present demonstration of significant disruption of intracellular Zn^{2+} homeostasis is another example of the significant impact of dialysis. The 20 minute dialysis conditions tested here are relatively common for studies of synaptic physiology or pathophysiology. The current results suggest that loss of Zn^{2+} buffering and/or intracellular release could be a significant variable in a range of whole-cell studies.

One of the most obvious dialysis effects was the response to low concentrations of the Zn^{2+} carrier Zn-pyrithione. As noted above, pyrithione serves to facilitate Zn^{2+} passage across the plasma membrane, and thereby increases intracellular Zn^{2+} levels independent of active transport mechanisms. The fact that standard intracellular dialysis significantly increased intracellular accumulation following Zn-pyrithione could be due to washout of intracellular buffers, or possibly due to some other factors that decrease Zn^{2+} extrusion rates. Reversal of the dialysis effect with recombinant MT3 is consistent with the possibility that washout of endogenous Zn^{2+} buffering proteins could underlie the dialysis effect, however increased endogenous Zn^{2+} buffer by MT3 inclusion could have masked dialysis effect on the other contributing mechanisms (e.g. decreased transporter/channel activity).

Likewise, the loss of intracellular Zn^{2+} accumulation following exposure of the oxidant DTDP is consistent with the hypothesis that dialysis washes out an oxidation-sensitive, diffusible Zn^{2+}-binding source, such as MT3. A similar role for metallothionein in intracellular Zn^{2+} buffering and regulating the oxidation sensitive pool size has previously been demonstrated with overexpression of metallothionein in astrocytes (Malaiyandi et al., 2004).

It is noteworthy that even in extensively dialyzed neurons, extremely low resting intracellular Zn^{2+} concentrations were detected by FluoZin-3 (estimated ~500 pM), which were not different from cells loaded with brief dialysis (see Figure 1). This suggests that mechanisms required for maintaining resting Zn^{2+} concentrations are different from those that prevent excessive intracellular Zn^{2+} accumulation. Thus while diffusible Zn^{2+} binding molecules (such as glutathione, thionein and metallothioneins) are likely important defense molecules against severe Zn^{2+} influx (Cho et al., 2003; Krezel and Maret, 2006), resting Zn^{2+} concentrations may not be under control of these molecules. It was recently reported that the functions of membrane Zn^{2+} transporters ZIP1 and ZIP3 are important in Zn^{2+} accumulation in CA1 pyramidal neurons (Qian et al., 2011), and those effects were observed in neurons with significant dialysis (30 minutes) implying that this pathway could remain intact. Thus mechanisms such as Zn^{2+} extrusion or sequestration into organelles alone could potentially be sufficient for maintaining extremely low Zn^{2+} concentrations at rest (Colvin et al., 2008; Sensi et al., 2009).

In addition to depletion of buffer molecules, the concentrations of small signaling molecules such as inositol phosphate can be modified by intracellular dialysis (Hourez et al., 2005). Because we did not replenish these small molecules, intracellular dialysis could have significantly impaired intracellular signaling pathways. For example, it was reported that Zn^{2+} dependent NMDAR potentiation by Src kinase is abolished by intracellular dialysis in cultured cortical neurons (Manzerra et al., 2001). These effects certainly could have

contributed to reduced detection of intracellular Zn^{2+} release in the dialyzed neurons, and facilitated selective detection of synaptic Zn^{2+} translocation in the dialyzed neurons.

In the current studies, dialysis was exploited to evaluate Zn^{2+} signals following synaptic stimulation, including influx from the extracellular space. However it is recognized that the same dialysis methods will likely influence cytosolic Zn^{2+} transients arising from other sources that are resistant to dialysis. Such sources could include intracellular compartments such as mitochondria, endoplasmic reticulum and lysosomes (see below) and Zn^{2+} transients arising from these sources may also be more readily detectable in extensively dialyzed cells.

3. Neuronal intracellular Zn^{2+} buffer systems

The present study revealed that inclusion of MT3 alone was sufficient to restore a large portion of intracellular Zn^{2+} homeostasis. However this does not necessarily rule out important contributions of other Zn^{2+} buffers. GSH provides an additional major cytoplasmic Zn^{2+} buffer in hippocampus (Sato et al., 1984), but as GSH is less abundant in neurons (1 mM) compared with the glia (10 mM) (Rice and Russo-Menna, 1998) this buffer may not play a major role in the neuronal signals examined here. In addition, it is known that GSH concentrations can be severely depleted during brain slice preparation (Rice, 1999). These and other factors might have made contributions of MT3 dialysis relatively more detectable in the brain slice preparations studied here.

Zn^{2+} binding to MT3 can be quite dynamic despite the high affinity of MT3 for Zn^{2+} leading to the simultaneous detection of differently Zn^{2+}-bound and -saturated forms (Palumaa et al., 2002; Palumaa et al., 2005). It has also been shown that MT3 contains weak Zn^{2+} binding sites which may become available in the presence of FluoZin-3 (Krezel and Maret, 2007). The present study examined effects of recombinant MT3 originally supplied as a mixture of Zn^{2+}-bound forms (see Methods). The fact that partially Zn^{2+}-saturated MT3 could act as both a sink (Figure 2) and a source of Zn^{2+} (Figure 3), is consistent with the idea that the protein remained only partially saturated with Zn^{2+} after dialysis, in FluoZin-3 containing conditions. A similar sink / source function of MT was previously demonstrated in astrocytes overexpressing MT2 (Malaiyandi et al., 2004) and has been suggested to explain differential effects of MT3 deletion in different injury models involving Zn^{2+} toxicity (see Discussion in Sheline et al., 2010).

The incomplete rescue by MT3 addition of Zn^{2+} responses in dialyzed neurons leaves open the possibility that the other Zn^{2+} sinks, such as mitochondria, endoplasmic reticulum, Golgi and lysosomes (Sensi et al., 2009; Lee and Koh, 2010) could contribute to shaping the FluoZin-3 transients seen here.

4. Intracellular Zn^{2+} responses during synaptic stimulation

Previous studies suggest that synaptic stimulation may elevate intracellular Zn^{2+} levels by two mechanisms; intracellular Zn^{2+} release and synaptic Zn^{2+} translocation (see introduction). Bulk loading of populations of CA1 neurons with a low affinity Zn^{2+} indicator Newport Green (K_D = 1~3 μM) (Li et al., 2001; Suh, 2009) has shown intracellular Zn^{2+} increases in postsynaptic neurons (Li et al., 2001; Suh, 2009) and the latter study showed that accumulation was abolished in ZnT3 KO tissues and by application of CaEDTA. While this suggested a major role of synaptic Zn^{2+} release and translocation, the results of the present study suggest that both synaptic release and intracellular release can contribute to postsynaptic Zn^{2+} accumulation at Schaffer collateral-CA1 synapses. Thus in briefly dialyzed preparations, postsynaptic Zn^{2+} responses were observed in both WT and ZnT3 KO preparations. The presence of responses in ZnT3 KO preparations suggest that, in our recording conditions, intracellular Zn^{2+} release can significantly contribute to the

FluoZin-3 signal changes following synaptic stimulation. Conversely with standard dialysis, FluoZin-3 signals were abolished in ZnT3 KO tissues, implying preferential detection of Zn^{2+} that is released and taken up by postsynaptic neurons. Taken together, the preferential detection of intracellular Zn^{2+} release in the briefly dialyzed neurons is likely contributed to by the presence of intracellular buffers, which bind with Zn^{2+} with significantly higher affinity and masked a large part of fluxed Zn^{2+} from detection by FluoZin-3. In addition, there was evidence for release of Zn^{2+} from recombinant MT3 by synaptic stimulation (compare Figure 4B&F). This may explain why inclusion of this MT3 did not prevent detection of synaptic Zn^{2+} translocation in extensively dialyzed neurons. While it has been previously shown that glutamate can evoke intracellular Zn^{2+} release in neuronal culture models (Sensi et al., 2003; Dineley et al., 2008; Kiedrowski, 2011), the present study appears to be the first to suggest intracellular Zn^{2+} release during physiological synaptic activity.

A number of experimental differences may underlie the differences between the present study, and the previous conclusion that synaptic translocation appeared entirely responsible for Zn^{2+} signals after electrical stimulation (Suh, 2009). Relevant differences include the delivery of the higher affinity indicator FluoZin-3 into single neurons, and use of CaEDTA in the superfusate to prevent detection of contaminating Zn^{2+} (see Discussion in Carter et al., 2011). Postsynaptic Zn^{2+} transients observed here were much faster than previously reported by Suh 2009, and these experimental conditions appear to favor detection of a combination of intracellular mobilization, as well as trans-synaptic flux.

We also noted that postsynaptic Zn^{2+} responses were completely abolished when glutamate receptors were blocked (see Supplementary Figure), regardless of the dialysis method used. These results are consistent with prior demonstration of glutamate receptor dependent intracellular release (Sensi et al., 2003; Dineley et al., 2008; Kiedrowski, 2012) and Zn^{2+} influx through glutamate/depolarization gated channels (e.g. voltage gated Ca^{2+} channel, AMPAR, NMDAR) (Sensi et al., 1997; Sensi et al., 1999; Kerchner et al., 2000; Sensi et al., 2000; Huang et al., 2008).

5. Kinetics of Zn^{2+} responses

One of the remarkable features of intracellular Zn^{2+} responses following synaptic stimulation is their very slow kinetics. Both in standard dialysis and briefly dialyzed preparations, similar slow monophasic responses were detected. The intracellular Zn^{2+} responses were much slower than intracellular Ca^{2+} transients observed with the same stimuli (data not shown). Previous single cell Zn^{2+} imaging during different stimuli (exposures to ouabain, oxygen glucose deprivation and NMDA) have also shown relatively slow changes in intracellular FluoZin-3 signals (Dietz et al., 2008; Medvedeva et al., 2009; Vander Jagt et al., 2009). One possible explanation for the slow kinetics is that high affinity endogenous intracellular Zn^{2+} buffers limit mobility of Zn^{2+} ions and contributed to sluggish responses. However our dialysis studies suggest this may not be a major contributor. In fact, similarly slow responses were also observed in the dialyzed neurons in which a large fraction of intracellular Zn^{2+} buffer is likely to be significantly depleted. Instead of large buffer molecules, these slow responses could be contributed by interactions with organic anions (e.g. HCO_3^-, PO_4^{3-}) which are abundantly present in the cytoplasm with high affinity (Rumschik et al., 2009). An interesting question is whether the observed responses may reflect true intracellular Zn^{2+} dynamics, or whether signals are distorted due to presence of fluorescence probes. Thus a high affinity Zn^{2+} binding molecule such as FluoZin-3 could significantly impact the mobility of Zn^{2+}. Because of extremely low intracellular Zn^{2+} concentrations at rest and even after stimulation, such a confound may be inevitable for imaging studies of intracellular Zn^{2+}.

6. Conclusion

The present study revealed significant effects on intracellular Zn^{2+} homeostasis by conditions used in standard electrophysiological experiments. The results also suggest that modifying whole cell indicator loading conditions can be valuable tool to help discriminate between different sources of Zn^{2+} that contribute to intracellular neuronal Zn^{2+} signals in adult brain slice preparations.

Supplementary Material

Refer to Web version on PubMed Central for supplementary material.

Acknowledgments

Supported by NIH grants NS051288 (C.W.S) & DK073446 (C.T.S), AHA grant 11PRE4870002 (I.A.). The authors thank Dr LD Partridge for helpful review of the manuscript.

Abbreviations

TPEN	(N,N,N′,N′-Tetrakis(2-pyridylmethyl)ethylenediamine
ZnPyr	zinc pyrithione
MT3	metallothionein 3
EGTA	Ethylene glycol tetraacetic acid

References

Aizenman E, Stout AK, Hartnett KA, Dineley KE, McLaughlin B, Reynolds IJ. Induction of neuronal apoptosis by thiol oxidation: putative role of intracellular zinc release. Journal of neurochemistry. 2000; 75:1878–1888. [PubMed: 11032877]

Blatow M, Caputi A, Burnashev N, Monyer H, Rozov A. Ca2+ buffer saturation underlies paired pulse facilitation in calbindin-D28k-containing terminals. Neuron. 2003; 38:79–88. [PubMed: 12691666]

Carter RE, Aiba I, Dietz RM, Sheline CT, Shuttleworth CW. Spreading depression and related events are significant sources of neuronal Zn2+ release and accumulation. Journal of cerebral blood flow and metabolism : official journal of the International Society of Cerebral Blood Flow and Metabolism. 2011; 31:1073–1084. [PubMed: 20978516]

Cho IH, Im JY, Kim D, Kim KS, Lee JK, Han PL. Protective effects of extracellular glutathione against Zn2+-induced cell death in vitro and in vivo. Journal of neuroscience research. 2003; 74:736–743. [PubMed: 14635224]

Choi DW, Koh JY. Zinc and brain injury. Annual review of neuroscience. 1998; 21:347–375.

Cole TB, Wenzel HJ, Kafer KE, Schwartzkroin PA, Palmiter RD. Elimination of zinc from synaptic vesicles in the intact mouse brain by disruption of the ZnT3 gene. Proceedings of the National Academy of Sciences of the United States of America. 1999; 96:1716–1721. [PubMed: 9990090]

Colvin RA, Bush AI, Volitakis I, Fontaine CP, Thomas D, Kikuchi K, Holmes WR. Insights into Zn2+ homeostasis in neurons from experimental and modeling studies. American journal of physiology Cell physiology. 2008; 294:C726–742. [PubMed: 18184873]

Dietz RM, Weiss JH, Shuttleworth CW. Zn2+ influx is critical for some forms of spreading depression in brain slices. The Journal of neuroscience : the official journal of the Society for Neuroscience. 2008; 28:8014–8024. [PubMed: 18685026]

Dineley KE, Devinney MJ 2nd, Zeak JA, Rintoul GL, Reynolds IJ. Glutamate mobilizes [Zn2+] through Ca2+-dependent reactive oxygen species accumulation. Journal of neurochemistry. 2008; 106:2184–2193. [PubMed: 18624907]

Eggermann E, Jonas P. How the ‘slow’ Ca(2+) buffer parvalbumin affects transmitter release in nanodomain-coupling regimes. Nature neuroscience. 2012; 15:20–22.

Frederickson CJ, Koh JY, Bush AI. The neurobiology of zinc in health and disease. Nature reviews Neuroscience. 2005; 6:449–462.

Gee KR, Zhou ZL, Qian WJ, Kennedy R. Detection and imaging of zinc secretion from pancreatic beta-cells using a new fluorescent zinc indicator. Journal of the American Chemical Society. 2002; 124:776–778. [PubMed: 11817952]

Grynkiewicz G, Poenie M, Tsien RY. A new generation of Ca2+ indicators with greatly improved fluorescence properties. The Journal of biological chemistry. 1985; 260:3440–3450. [PubMed: 3838314]

Hall CN, Klein-Flugge MC, Howarth C, Attwell D. Oxidative phosphorylation, not glycolysis, powers presynaptic and postsynaptic mechanisms underlying brain information processing. The Journal of neuroscience : the official journal of the Society for Neuroscience. 2012; 32:8940–8951. [PubMed: 22745494]

Hidalgo J, Garcia A, Oliva AM, Giralt M, Gasull T, Gonzalez B, Milnerowicz H, Wood A, Bremner I. Effect of zinc, copper and glucocorticoids on metallothionein levels of cultured neurons and astrocytes from rat brain. Chemico-biological interactions. 1994; 93:197–219. [PubMed: 7923440]

Hourez R, Azdad K, Vanwalleghem G, Roussel C, Gall D, Schiffmann SN. Activation of protein kinase C and inositol 1,4,5-triphosphate receptors antagonistically modulate voltage-gated sodium channels in striatal neurons. Brain research. 2005; 1059:189–196. [PubMed: 16168392]

Huang YZ, Pan E, Xiong ZQ, McNamara JO. Zinc-mediated transactivation of TrkB potentiates the hippocampal mossy fiber-CA3 pyramid synapse. Neuron. 2008; 57:546–558. [PubMed: 18304484]

Kerchner GA, Canzoniero LM, Yu SP, Ling C, Choi DW. Zn2+ current is mediated by voltage-gated Ca2+ channels and enhanced by extracellular acidity in mouse cortical neurones. The Journal of physiology. 2000; 528(Pt 1):39–52. [PubMed: 11018104]

Kiedrowski L. Cytosolic zinc release and clearance in hippocampal neurons exposed to glutamate--the role of pH and sodium. Journal of neurochemistry. 2011; 117:231–243. [PubMed: 21255017]

Kiedrowski L. Cytosolic acidification and intracellular zinc release in hippocampal neurons. Journal of neurochemistry. 2012; 121:438–450. [PubMed: 22339672]

Krezel A, Maret W. Zinc-buffering capacity of a eukaryotic cell at physiological pZn. Journal of biological inorganic chemistry : JBIC : a publication of the Society of Biological Inorganic Chemistry. 2006; 11:1049–1062. [PubMed: 16924557]

Krezel A, Maret W. Dual nanomolar and picomolar Zn(II) binding properties of metallothionein. Journal of the American Chemical Society. 2007; 129:10911–10921. [PubMed: 17696343]

Krezoski SK, Villalobos J, Shaw CF 3rd, Petering DH. Kinetic lability of zinc bound to metallothionein in Ehrlich cells. The Biochemical journal. 1988; 255:483–491. [PubMed: 3202828]

Lavoie N, Peralta MR 3rd, Chiasson M, Lafortune K, Pellegrini L, Seress L, Toth K. Extracellular chelation of zinc does not affect hippocampal excitability and seizure-induced cell death in rats. The Journal of physiology. 2007; 578:275–289. [PubMed: 17095563]

Lee SJ, Koh JY. Roles of zinc and metallothionein-3 in oxidative stress-induced lysosomal dysfunction, cell death, and autophagy in neurons and astrocytes. Molecular brain. 2010; 3:30. [PubMed: 20974010]

Li Y, Hough CJ, Suh SW, Sarvey JM, Frederickson CJ. Rapid translocation of Zn(2+) from presynaptic terminals into postsynaptic hippocampal neurons after physiological stimulation. Journal of neurophysiology. 2001; 86:2597–2604. [PubMed: 11698545]

Malaiyandi LM, Dineley KE, Reynolds IJ. Divergent consequences arise from metallothionein overexpression in astrocytes: zinc buffering and oxidant-induced zinc release. Glia. 2004; 45:346–353. [PubMed: 14966866]

Malinow R, Tsien RW. Presynaptic enhancement shown by whole-cell recordings of long-term potentiation in hippocampal slices. Nature. 1990; 346:177–180. [PubMed: 2164158]

Manzerra P, Behrens MM, Canzoniero LM, Wang XQ, Heidinger V, Ichinose T, Yu SP, Choi DW. Zinc induces a Src family kinase-mediated up-regulation of NMDA receptor activity and excitotoxicity. Proceedings of the National Academy of Sciences of the United States of America. 2001; 98:11055–11061. [PubMed: 11572968]

Medvedeva YV, Lin B, Shuttleworth CW, Weiss JH. Intracellular Zn2+ accumulation contributes to synaptic failure, mitochondrial depolarization, and cell death in an acute slice oxygen-glucose deprivation model of ischemia. The Journal of neuroscience : the official journal of the Society for Neuroscience. 2009; 29:1105–1114. [PubMed: 19176819]

Palumaa P, Eriste E, Njunkova O, Pokras L, Jornvall H, Sillard R. Brain-specific metallothionein-3 has higher metal-binding capacity than ubiquitous metallothioneins and binds metals noncooperatively. Biochemistry. 2002; 41:6158–6163. [PubMed: 11994011]

Palumaa P, Tammiste I, Kruusel K, Kangur L, Jornvall H, Sillard R. Metal binding of metallothionein-3 versus metallothionein-2: lower affinity and higher plasticity. Biochimica et biophysica acta. 2005; 1747:205–211. [PubMed: 15698955]

Pan E, Zhang XA, Huang Z, Krezel A, Zhao M, Tinberg CE, Lippard SJ, McNamara JO. Vesicular zinc promotes presynaptic and inhibits postsynaptic long-term potentiation of mossy fiber-CA3 synapse. Neuron. 2011; 71:1116–1126. [PubMed: 21943607]

Qian J, Noebels JL. Visualization of transmitter release with zinc fluorescence detection at the mouse hippocampal mossy fibre synapse. The Journal of physiology. 2005; 566:747–758. [PubMed: 15919713]

Qian J, Xu K, Yoo J, Chen TT, Andrews G, Noebels JL. Knockout of Zn transporters Zip-1 and Zip-3 attenuates seizure-induced CA1 neurodegeneration. The Journal of neuroscience : the official journal of the Society for Neuroscience. 2011; 31:97–104. [PubMed: 21209194]

Rice ME. Use of ascorbate in the preparation and maintenance of brain slices. Methods. 1999; 18:144–149. [PubMed: 10356344]

Rice ME, Russo-Menna I. Differential compartmentalization of brain ascorbate and glutathione between neurons and glia. Neuroscience. 1998; 82:1213–1223. [PubMed: 9466441]

Rumschik SM, Nydegger I, Zhao J, Kay AR. The interplay between inorganic phosphate and amino acids determines zinc solubility in brain slices. Journal of neurochemistry. 2009; 108:1300–1308. [PubMed: 19183267]

Sakmann B, Neher E. Patch clamp techniques for studying ionic channels in excitable membranes. Annual review of physiology. 1984; 46:455–472.

Sato SM, Frazier JM, Goldberg AM. The distribution and binding of zinc in the hippocampus. The Journal of neuroscience : the official journal of the Society for Neuroscience. 1984; 4:1662–1670. [PubMed: 6726351]

Sensi SL, Yin HZ, Weiss JH. AMPA/kainate receptor-triggered Zn2+ entry into cortical neurons induces mitochondrial Zn2+ uptake and persistent mitochondrial dysfunction. The European journal of neuroscience. 2000; 12:3813–3818. [PubMed: 11029652]

Sensi SL, Ton-That D, Weiss JH. Mitochondrial sequestration and Ca(2+)-dependent release of cytosolic Zn(2+) loads in cortical neurons. Neurobiology of disease. 2002; 10:100–108. [PubMed: 12127148]

Sensi SL, Paoletti P, Bush AI, Sekler I. Zinc in the physiology and pathology of the CNS. Nature reviews Neuroscience. 2009; 10:780–791.

Sensi SL, Yin HZ, Carriedo SG, Rao SS, Weiss JH. Preferential Zn2+ influx through Ca2+-permeable AMPA/kainate channels triggers prolonged mitochondrial superoxide production. Proceedings of the National Academy of Sciences of the United States of America. 1999; 96:2414–2419. [PubMed: 10051656]

Sensi SL, Canzoniero LM, Yu SP, Ying HS, Koh JY, Kerchner GA, Choi DW. Measurement of intracellular free zinc in living cortical neurons: routes of entry. The Journal of neuroscience : the official journal of the Society for Neuroscience. 1997; 17:9554–9564. [PubMed: 9391010]

Sensi SL, Ton-That D, Sullivan PG, Jonas EA, Gee KR, Kaczmarek LK, Weiss JH. Modulation of mitochondrial function by endogenous Zn2+ pools. Proceedings of the National Academy of Sciences of the United States of America. 2003; 100:6157–6162. [PubMed: 12724524]

Sheline CT, Cai AL, Zhu J, Shi C. Serum or target deprivation-induced neuronal death causes oxidative neuronal accumulation of Zn2+ and loss of NAD+ The European journal of neuroscience. 2010; 32:894–904. [PubMed: 20722716]

Suh SW. Detection of zinc translocation into apical dendrite of CA1 pyramidal neuron after electrical stimulation. Journal of neuroscience methods. 2009; 177:1–13. [PubMed: 18929598]

Vander Jagt TA, Connor JA, Weiss JH, Shuttleworth CW. Intracellular Zn2+ increases contribute to the progression of excitotoxic Ca2+ increases in apical dendrites of CA1 pyramidal neurons. Neuroscience. 2009; 159:104–114. [PubMed: 19135505]

Vogt K, Mellor J, Tong G, Nicoll R. The actions of synaptically released zinc at hippocampal mossy fiber synapses. Neuron. 2000; 26:187–196. [PubMed: 10798403]

West AK, Hidalgo J, Eddins D, Levin ED, Aschner M. Metallothionein in the central nervous system: Roles in protection, regeneration and cognition. Neurotoxicology. 2008; 29:489–503. [PubMed: 18313142]

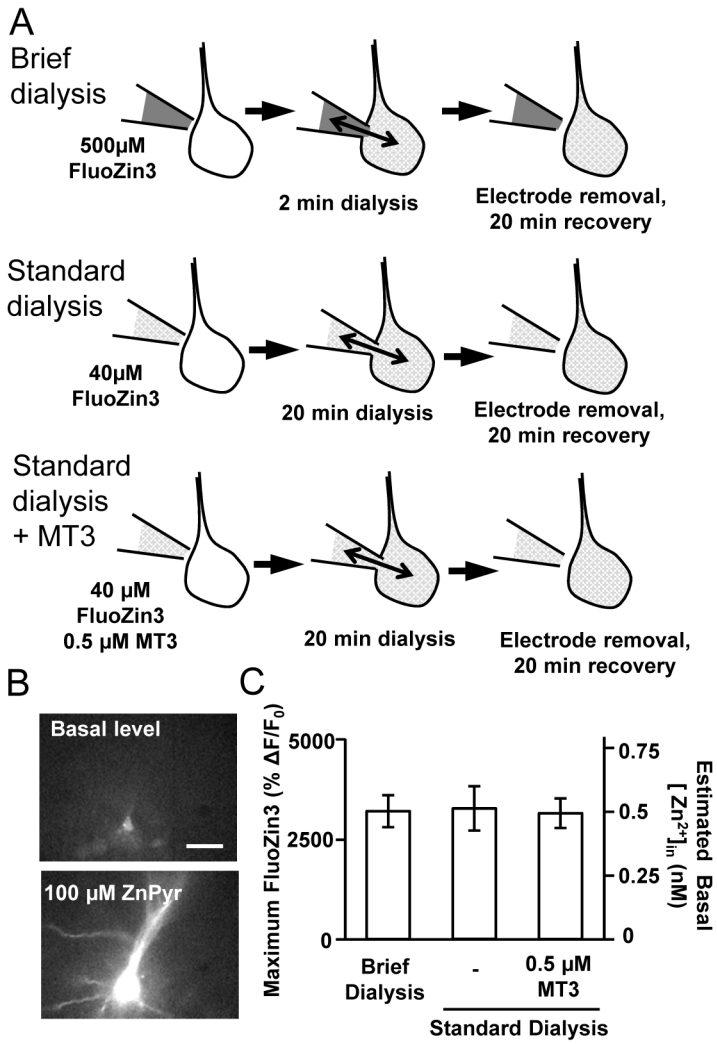

Figure 1. Experimental approach for FluoZin-3 loading

The high affinity Zn^{2+} indicator FluoZin3 was loaded into hippocampal CA1 pyramidal neurons in acute brain slices via patch-pipettes. **A:** Three different intracellular loading methods are illustrated; Brief dialysis (2min, *top*), Standard dialysis (20 min, *middle*) and Standard dialysis supplemented with 0.5 μM MT3 (20 min, *bottom*). Pipette concentrations of FluoZin-3 were adjusted to achieve similar final intracellular indicator concentrations with the different loading durations (500μM or 40μM, as indicated). **B:** Representative images of a briefly-dialyzed neuron, showing FluoZin-3 increases before and after challenge with a saturating concentration of the Zn^{2+} ionophore complex ZnPyr (100 μM $ZnCl_2$ and 5 μM pyrithione). Scale bar: 40 μm. Similar challenges with ZnPyr were used to estimate basal intracellular Zn^{2+} concentrations shown in C. **C:** Comparisons of maximum fluorescence signals generated by saturating concentrations of ZnPyr (100 μM $ZnCl_2$ and 5 μM pyrithione) in the three recording conditions. The left hand axis shows recorded peak FluoZin3 signals, and the right hand axis shows estimated basal Zn^{2+} concentrations (see Methods). No significant differences were seen ($p>0.05$, $n=5$ each).

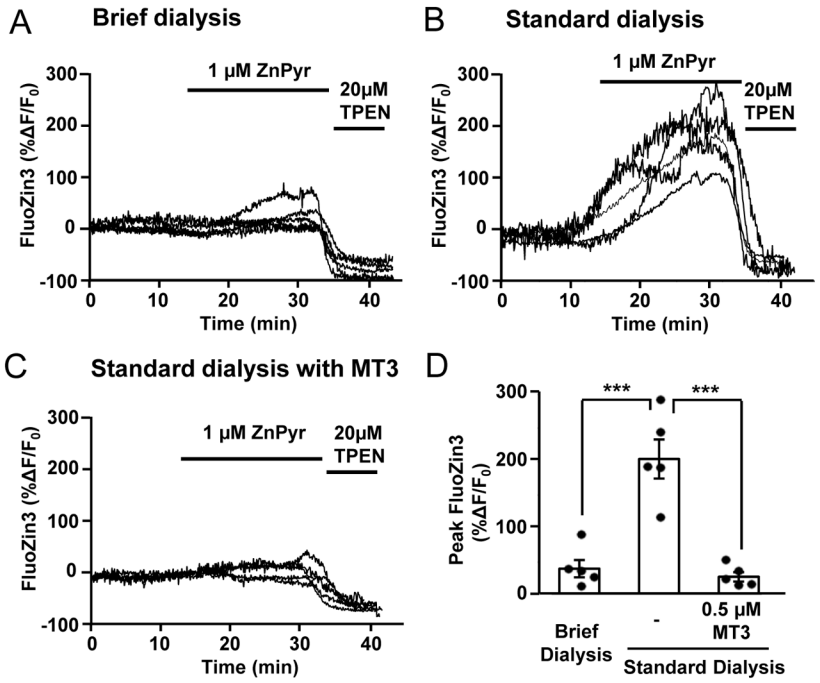

Figure 2. Intracellular dialysis strongly modifies detection of intracellular Zn^{2+} following exposure to ZnPyr

FluoZin-3-loaded neurons were exposed to 1 μM ZnPyr (1 μM $ZnCl_2$ and 1 μM sodium pyrithione, 20 minutes), followed by 20 μM TPEN. **A–C** Plots of responses from 5 individual neurons, with either brief dialysis (**A:** 2 minutes), standard dialysis (**B:** 20 minutes) or standard dialysis supplemented with recombinant MT3 (**C**). **D.** Quantitative analysis of peak FluoZin-3 responses. ***p<0.005.

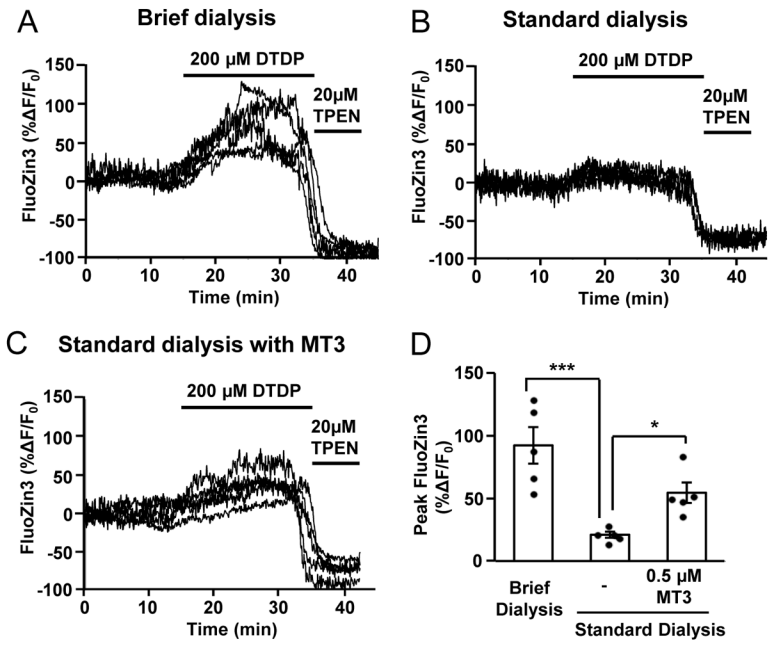

Figure 3. Brief dialysis maintains oxidant-sensitive intracellular Zn^{2+} pool size

FluoZin-3-loaded loaded neurons were challenged with ACSF containing 200 μM DTDP. After significant Zn^{2+} responses were obtained, neurons were then exposed to 20 μM TPEN. **A–C** shows responses from 5 individual neurons under the same conditions as described in Figure 2, and **D** shows a quantitative analysis of peak responses. ***p<0.005

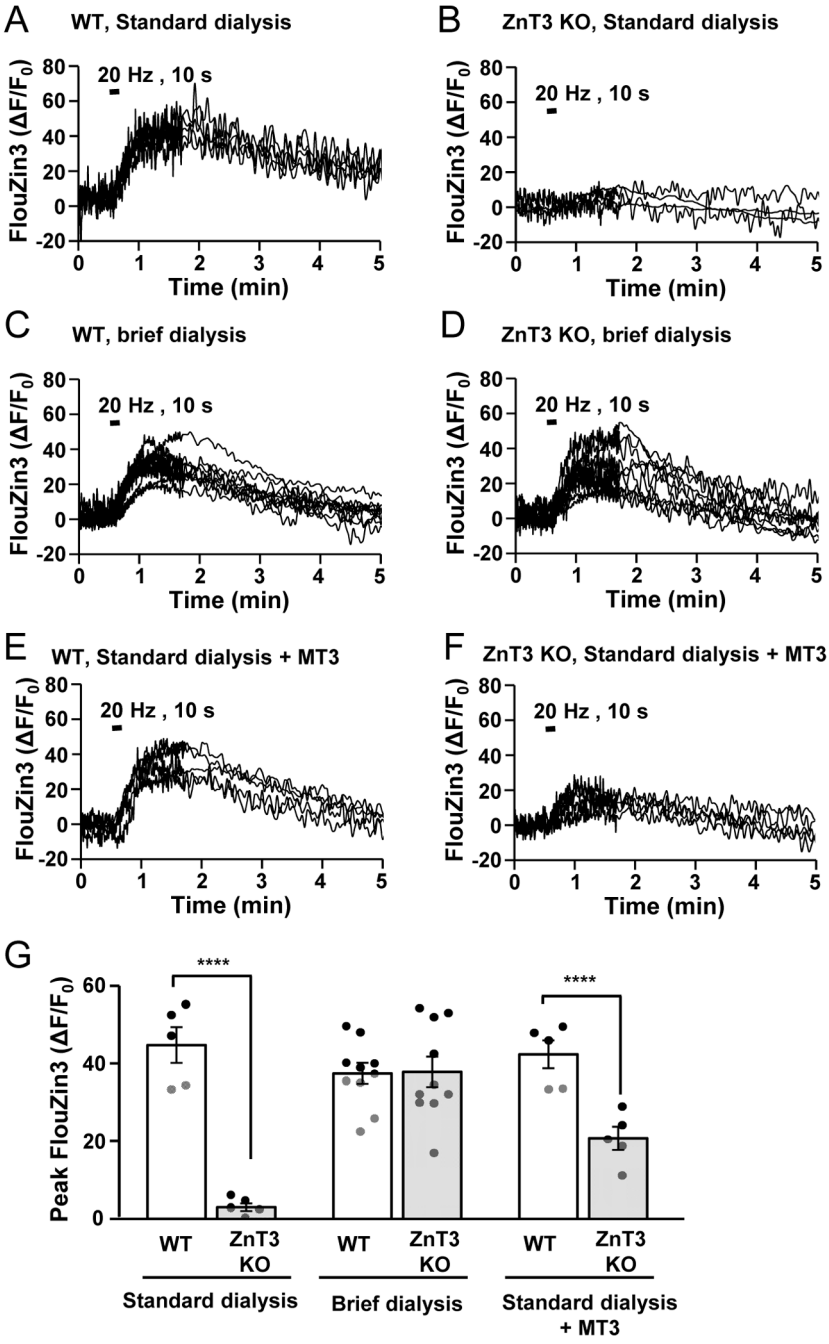

Figure 4. Manipulation of intracellular dialysis can be used to implicate both intracellular release and transmembrane Zn^{2+} flux to postsynaptic Zn^{2+} accumulation following synaptic stimulation

FluoZin-3 loaded neurons from WT and ZnT3 KO slices are shown, with three different intracellular dialysis methods. Following recovery slices were challenged with Schaffer collateral synaptic stimulation (20 Hz, 10 s). Panels **A–F** shows individual responses obtained from multiple neurons in each preparation (n=10 for brief dialysis, n=5 for all others). Note that the acquisition rate was changed after 1.6 min (from 2Hz to 0.4Hz) in each recording. Peak responses were obtained following data-reduced traces and are compared in **G**. ***p<0.005